Identification of essential genes for *Escherichia coli* aryl polyene biosynthesis and function in biofilm formation

Isabel Johnston[1], Lucas J Osborn[1], Elizabeth A McManus[1,2], Anagha Kadam[1], Karlee B Schultz[1,3], Philip P Ahern[1,4], J Mark Brown[1,4], Jan Claesen[1,4]*

[1]Department of Cardiovascular and Metabolic Sciences, Lerner Research Institute, Cleveland Clinic, Cleveland, OH, USA

[2]Current affiliation: National Cancer Institute, National Institutes of Health, Bethesda, MD, USA

[3]College of Arts and Sciences, John Carroll University, University Heights, OH, USA

[4]Center for Microbiome and Human Health, Cleveland Clinic, Cleveland, OH, USA

*Correspondence to: claesej@ccf.org

ABSTRACT

Aryl polyenes (APEs) are specialized polyunsaturated lipids that were identified *in silico* as the product of the most widespread family of bacterial biosynthetic gene clusters (BGCs). They are present in several Gram-negative host-associated bacteria, including multi-drug resistant human pathogens. Here, we characterize the biological function of APEs, focusing on the BGC from a uropathogenic *Escherichia coli* (UPEC) strain. We first perform a genetic deletion analysis to identify the essential genes required for APE biosynthesis. Next, we show that APEs function as fitness factors that increase protection from oxidative stress and contribute to biofilm formation. Together, our study highlights key steps in the APE biosynthesis pathway that can be explored as potential drug targets for complementary strategies to reduce fitness and prevent biofilm formation of multi-drug resistant pathogens.

MAIN TEXT

In a global search for novel types of bacterial secondary metabolites, we previously identified aryl polyenes (APEs) as the products of the most abundantly present biosynthetic gene cluster (BGC) family [1]. APEs are present in most major bacterial genera throughout the Proteobacteria and Bacteroidetes. They are often found in host-associated bacteria, including commensals as well as pathogens of humans, animals, and plants [1]. Among these are several human pathogens that are a major concern in nosocomial multidrug-resistant infections, including *Acinetobacter baumannii*, *Burkholderia cenocepacia*, as well as several *Enterobacter* isolates [2, 3]. APE BGCs are also present in most types of pathogenic *E. coli*, whereas they are typically absent from commensal and laboratory strains of *E. coli* [1].

APEs produced by diverse bacterial genera share a remarkably similar chemical scaffold, consisting of an aryl head group conjugated to a polyene carboxylic acid tail [1, 4-7] (Fig. 1). The main differences between APEs of different bacterial genera are in the polyene chain length and in the hydroxylation, methylation, or alkylation of the head group. This structural similarity is reflected in the observation that phylogenetically diverse APE BGCs share conserved core gene functions, resembling biosynthesis machinery for fatty acids and type II polyketides. Notably, an *in silico* comparison between BGCs identified differences in enzyme functions involved in alternative biosynthesis initiation, cell envelope attachment, and head group tailoring. Heterologous expression of the BGCs from *E. coli* CFT073 (APE_{Ec}) and *Vibrio fischeri* ES114 (APE_{Vf}) confirmed that these BGCs encompass all genes required for APE biosynthesis [1]. Moreover, the biosynthesis of the core APE moiety from the nematode symbiont *Xenorhabdus doucetiae* DSM17909 (APE_{Xd}) was recently reconstituted *in vitro* by Grammbitter *et al.* [8]. The functions of nine enzymes from the APE_{Xd} BGC were characterized after heterologous expression and purification from *E. coli* and used to form APE_{Xd} *in vitro*. Our current study addresses outstanding questions in APE biology, including the identity of the essential genes for *in vivo* biosynthesis and uncovering their biological function among the bacteria that produce them.

Gram-positive bacterial pathogens attach different types of polyenes in their cell envelope, including staphyloxanthin and granadaene (Fig. 1), which are polyenic virulence factors localized in the cell envelope of *Staphylococcus aureus* and Group B *Streptococcus*, respectively [9, 10]. Staphyloxanthin is a ‘golden’ carotenoid pigment, produced from the mevalonate pathway and granadaene is a red ornithine rhamno-polyene produced by fatty acid-like biosynthetic machinery [9, 10]. Despite their different biosynthetic origins, both of these compounds share remarkable analogous functions: they protect their producers from damage induced by reactive oxygen species (ROS) [11, 12]. Exogenous ROS can originate from a variety of sources, such as UV light, certain antibiotics or the host immune system. Neutrophils and macrophages utilize ROS

production as a critical component of the initial line of defense against invading bacterial pathogens [13]. The lethal effect of ROS can be attributed to widespread damage to bacterial cells, inducing DNA double strand breaks, as well as oxidation of proteins and lipids [14, 15]. Polyenes that are localized in the cell envelope can scavenge external ROS, thereby preventing more extensive damage to essential cellular molecules and increasing bacterial fitness. Hence, characterization of the staphyloxanthin biosynthetic pathway has fueled the development of an anti-virulence strategy for managing *S. aureus* infections [16].

APEs are covalently attached in the Gram-negative outer membrane this creating the potential to alter interactions between these bacteria and the surrounding environment. Among the best studied bacterial lifestyle changes that involve alterations in the expression of cell envelope structures are aggregation, adhesion to surfaces, and biofilm formation. Biofilms form when bacteria switch from planktonic growth to an adherent, three dimensional lifestyle by embedding themselves in a self-produced extracellular matrix [17]. Biofilm formation has impacts on bacterial physiology, affecting pathogenesis and antibiotic resistance. Decreased antibiotic susceptibility can be due to a slowing of bacterial growth and metabolic activity, as well as reduced ability of the molecules to penetrate the biofilm matrix and reach interior cells [18, 19]. Moreover, growth in biofilms is associated with horizontal gene transfer, leading to more rapid strain adaptation and evolution. Since pathogens are more resilient when growing in biofilms, understanding the underlying mechanisms of biofilm formation and devising strategies to prevent and eliminate this process represent an important approach to limiting their pathogenic effects.

In this study, we focus on the functional characterization of the APE_{Ec} BGC from uropathogenic *E. coli*. Using a heterologous expression and gene deletion approach, we identify the genes in the BGC that are required for APE_{Ec} biosynthesis. Bacterial strains that express APE_{Ec} are conferred with a fitness advantage compared to their APE^- counterparts. APE_{Ec} producers have an increased viability when subjected to an acute oxidative stress challenge and have an increased capability to form biofilms. Our work marks an important step in the biological understanding of APE_{Ec} function and paves the way for the development of complementary strategies to reduce *in vivo* fitness and biofilm formation of multidrug-resistant human pathogens.

RESULTS

The *E. coli* APE_{Ec} BGC contains predicted redundant functions and a dedicated transport system

We previously identified APEs as the product of one of the most abundant bacterial BGC families and chose the BGC from *E. coli* CFT073 for in-depth characterization. Heterologous expression of this 18 gene, 15.5 kb BGC showed that this region contains all the genes required for production of APE_{Ec} (Fig. 2, [1]). All genes in the cluster are in the same orientation and several have overlapping open reading frames, suggesting the cluster is transcribed as one or multiple polycistronic mRNAs. The APE_{Ec} BGC encodes some seemingly duplicated functions, for example there are two acyl carrier proteins (ACPs, ApeE and F), two 3-hydroxyacyl-ACP dehydratases (ApeI and P) and three 3-ketoacyl-ACP synthases (ApeC, O and R, Fig. 2, Table 1). *In vitro* studies by Grammbitter *et al.* [8] on the APE_{Xd} BGC showed that ApeR is required for initiation and that ApeC functions as a chain length factor through heterocomplex formation with ApeO, which is responsible for chain elongation. Interestingly, the ApeC chain length factor is encoded near the beginning of the cluster, whereas most of the other core biosynthesis genes are located quite distantly, near the cluster's end.

The APE_{Ec} biosynthetic pathway is predicted to start with the activation of 4-hydroxybenzoic acid (4-HBA) by the specialized acyl-ACP synthetase ApeH (Fig. 3). *In vitro* reconstitution of the ApeH activity from the APE_{Xd} BGC revealed that this enzyme is capable of 4-HBA adenylation and ACP-loading without the formation of an intermediate CoA-thioester [8]. In *E. coli* and other Gram-negative bacteria, 4-HBA is produced by chorismate lyase (UbiC) as the first step in the ubiquinone biosynthesis pathway [20]. The APE_{Ec} cluster does not contain a dedicated phosphopantetheinyl transferase (PPTase) to activate the ACPs, ApeEF. An orphan PPTase, AcpT, was previously identified in *E. coli* O157:H7 EDL933, and *in vitro* biochemical analysis showed it can activate the respective ApeEF homologues in that strain [21]. The aromatic starter is further elongated with malonyl-ACP units by repetitive action of core biosynthetic enzymes related to those involved in fatty-acid and type II polyketide biosynthesis (Fig. 3). Methylation of the APE_{Ec} aromatic head group is likely catalyzed by the S-adenosyl-L-methionine dependent methyltransferase ApeB. The putative thioesterase ApeK could be involved in assisting the release of the finished APE_{Ec}-carboxylic acid from the ACP. Finally, APE_{Ec} is predicted to be acylated to a larger molecular entity in the membrane by two acyltransferases, ApeD and ApeJ, possibly via a glycerophospholipid-derived intermediate.

Gram-negative lipid biosynthesis requires adenosine triphosphate (ATP) and therefore typically takes place at the inner leaflet of the cell membrane. Lipids that are destined for the outer membrane are subsequently transported across the periplasm by dedicated transport systems [22]. The remaining genes in the APE_{Ec} BGC have no predicted biosynthetic or regulatory function and sequence-based homology searches suggest they might be involved in transport to the outer membrane. ApeM belongs to the COG4258 superfamily, which includes “Mycobacterial membrane protein Large (MmpL)” transporters which participate in lipid export to the Mycobacterial outer membrane [23]. ApeG is a membrane protein with a predicted COG468 pyrophosphatase domain that could be involved in providing the energy to drive transport through ATP hydrolysis. ApeL and ApeN share weak homology to components of the ‘localization of lipoprotein’ (Lol) pathway [22, 24], and these could be involved in localization of the predicted lipoprotein ApeA to the outer membrane. ApeGLMN homologs are conserved across different APE BGCs [1], suggesting they constitute dedicated transport machinery with low similarity to currently characterized translocation systems.

Genetic analysis of the APE_{Ec} BGC reveals essential biosynthesis genes

We have constructed deletion mutants to link the individual genes in the APE_{Ec} BGC to their role in the biosynthetic pathway and identify potential functionally redundant genes *in vivo* (Table 1). To avoid potential polar effects of gene deletions within polycistronic operons, we used an in-frame “scarred” strategy involving a two-step PCR-generated recombineering procedure (Fig. S1, [25]). In the first step, the coding sequence between the start and stop codon for a gene of interest is replaced using a PCR cassette containing an antibiotic resistance marker with flanking FRT sites and homologous regions to the target gene. For overlapping genes, we designed in-frame deletion constructs that keep the entire overlapping open reading frame intact. In the second step, Flp recombinase is used to excise the resistance marker by recombining the FRT sites. In the resulting deletion mutant, the gene’s coding region is replaced by an in-frame 81 nucleotide “scar” sequence that lacks stop codons in all reading frames, thereby avoiding potential polar effects on downstream genes.

Upon heterologous introduction of the 15.5 kb APE_{Ec} BGC in a standard *E. coli* Top10 cloning strain (devoid of native BGC), we observed a strong yellow pigmentation phenotype [1]. Since APEs are covalently attached to the outer membrane, pigmentation is cell-associated and does

not diffuse out into the culture medium. We used cell pellet pigmentation as a read-out for APE_{Ec} pathway functionality: mutant plasmids that conferred wild-type level pigmentation, comparable to the pJC121 containing parent strain are designated APE^+; mutant plasmids that conferred reduced pigmentation are $APE^{\pm}$; and mutant plasmids that did not display any pigmentation and thus were comparable to *E. coli* Top10 harboring the SuperCosI empty vector control were designated APE^- (Fig. 2). As expected, most mutants in predicted core biosynthetic genes (represented in shades of blue in Fig. 2) are APE^-. Only deletion of *apeA*, the first gene in the BGC, retains wild type levels of pigmentation, suggesting it is not required for APE_{Ec} biosynthesis. Surprisingly, the methyltransferase mutant Δ*apeB* was non-pigmented and deletion of one of the two ACPs, Δ*apeF*, retains partial pigmentation. Both acyltransferase mutants, Δ*apeD* and Δ*apeJ*, are $APE^{\pm}$ as well. The latter observation suggests the formation of molecular entities that are intermediates in the cell envelope attachment process. We did not obtain scarred deletion mutants for *apeL*, *apeN* or *apeO* and the APE^- phenotype of their respective $\Delta apra^R$ mutants could be due to polar effects on essential downstream genes in the BGC (Fig. 2). In summary, individual deletions in most of the core biosynthesis and transport genes abolished APE-associated pigmentation, whereas deletion of genes that are predicted to occur later in the pathway result in reduced pigmentation that could be caused by reduced flux through the pathway and improperly attached APE_{Ec} intermediates.

APE_{Ec} confers increased protection from oxidative challenge

Inspired by studies showing that staphyloxanthin deletion mutants of *S. aureus* are more susceptible to ROS [11, 26], we hypothesized that APEs fulfill a similar role for their Gram-negative producers. To test for protection against acute ROS stress, we compared APE^+ and APE^- *E. coli* resilience in a hydrogen peroxide (H_2O_2) survival assay (Fig. 4). Bacteria from an overnight liquid culture were challenged with incremental concentrations of H_2O_2 for one hour, after which the reaction was quenched by addition of excess catalase. Dilutions of the reaction mixtures were plated to count colony forming units and percent survival was calculated relative to the phosphate buffered saline (PBS) control incubation without added H_2O_2. At higher H_2O_2 concentrations, the APE^+ strain had a significant fitness advantage compared to APE^-. We next set out to determine whether APE expression confers a difference in the minimal inhibitory concentration (MIC) of H_2O_2. We observed a modest difference in MIC of 50 µM for APE^+ compared to 25 µM for APE^-. Our data suggest that APE_{Ec} expression can protect bacteria against acute ROS stress, such as from an oxidative burst but that APE_{Ec} production does not confer a significant advantage over longer periods of exposure.

Expression of the APE_{Ec} BGC induces biofilm formation

We observed that APE^+ bacteria form aggregates when grown in liquid culture and we hypothesized that the presence of APE_{Ec} in the outer membrane affects biofilm formation. To test this, we assessed the biofilm formation capacity of *E. coli* APE^- and APE^+ in an *in vitro* biofilm assay. The individual strains were grown in non-treated, flat-bottom plates for 48 hours and subsequently stained with crystal violet and quantified by measuring optical absorbance levels at 595 nm. We observed a marked increase in biofilm formation for the APE^+ strain (Fig. 5). To further characterize the biofilm structure and formation process over time, we visualized the biofilms at 48 and 72 hours using confocal fluorescence microscopy. This confirmed that the APE^+ strain forms a robust and homogenous biofilm after 48 hours, in comparison to the disperse attachment observed for APE^- (Fig. 6A). However, after 72 hours, there is no discernable difference between APE^+ and APE^- strains by confocal microscopy. In order to further investigate this finding, we recorded z-stacked images to assess the homogeneity and density of the

respective biofilms. Three-dimensional rendering of these images shows that APE_{Ec} expression results in a much thicker biofilm of ~60 µm, compared to the ~29 µm thick APE^- aggregates. At 72 hours, the APE^- biofilm becomes more homogenous in structure, but at ~46 µm remains thinner than the denser ~53 µm APE^+ biofilm. In conclusion, APE_{Ec} expression increases the rate of *E. coli* adherence and biofilm formation, resulting in a thicker and denser structure.

DISCUSSION

We report the first genetic characterization and functional analysis of an APE BGC from a medically relevant bacterial uropathogen. The core biosynthesis for APE_{Xd}, the product of a related BGC from the nematode symbiont *X. doucetiae*, was elucidated in a recent herculean *in vitro* effort by Grammbitter *et al.* [8]. Nine enzymes from the APE_{Xd} BGC (ApeC, E, F, H, I, O, P, Q and R) were produced heterologously in *E. coli* and several of these were found to form stable heterocomplexes. The biosynthetic roles for these enzymes were characterized and the formation of APE_{Xd}-ACP was reconstituted *in vitro*. Our genetic analysis of the *E. coli* CFT073 APE_{Ec} BGC complements this biochemical analysis and contributes important *in vivo* insights into the APE biosynthetic process, including the identification of functionally redundant core biosynthetic genes, as well as non-essential genes for cell envelope attachment and transport later in the pathway.

Among the mutants in the core biosynthetic genes, Δ*apeE* is APE^-, while Δ*apeF* retains partial pigmentation (Fig. 2), indicating that this latter ACP might be involved in malonyl chain extension and that the deletion could be partially complemented by the ACP involved in *E. coli* fatty acid biosynthesis, AcpP [27]. This also suggests that ApeF does not load 4-HBA *in vivo*, making ApeE the preferred ACP used for loading the 4-HBA starter (Figs. 2, 3). This observation is different from the prior *in vitro* reconstitution of the respective APE_{Xd} pathway, which showed that both ACPs could be loaded with 4-HBA, albeit at a much lower efficiency for ApeF [8]. Our deletion analysis indicates that this does not occur at sufficiently high levels for *in vivo* pathway activity. Moreover, the functional redundancy of ApeF is further illustrated by the observation that not all APE BGCs have a second ACP as is the case for xanthomonadin APE BGCs from *Xanthomonas spp.* [1, 28]. The APE^- pigmentation phenotype of the Δ*apeB* methyltransferase mutant was surprising given the enzyme's predicted function later in the pathway. One possible explanation for this observation is that ApeB acts earlier by methylating the 4-HBA starter. However, this seems unlikely since Grammbitter *et al.* demonstrated a broad *in vitro* substrate tolerance for ApeH [8]. Deletion of *apeK*, the gene encoding a putative thioesterase, resulted only in partial loss of pigmentation. No *in vitro* hydrolysis of 4-HBA-CoA or ACP-APE intermediates was observed for this enzyme, and a proofreading activity for ACP loading was proposed [8]. Since APE_{Ec} production wasn't abolished *in vivo*, this suggests that the putative proofreading activity is not absolutely required for biosynthesis but could have an impact on yield.

Several of the genes predicted to be involved in APE_{Ec} export and cell envelope attachment still produce reduced pigmentation upon knockout, suggesting the biosynthesis of the APE_{Ec} moiety is not disturbed and that this can lead to the accumulation of intermediates. At present, the identity of the molecule that covalently anchors APE_{Ec} in the outer membrane is still not known. Conserved domains in the two acyltransferases ApeD and ApeJ suggests that this molecular anchor could be a glycolipid, potentially lipid A or a derivative thereof. Alternatively, the presence of a predicted lipoprotein and Lol-like transport genes could imply that APEs might get localized to the outer membrane while serving as a lipid anchor for ApeA. This latter hypothesis seems less likely given the APE+ pigmentation phenotype of Δ*apeA*, indicating this gene is non-essential.

The generation of ROS constitutes a critical component of the initial line of defense by phagocytes against invading bacterial pathogens [13]. In turn, bacteria have developed several mechanisms to protect themselves from ROS damage. Enzymatic detoxification is an important mechanism employed to deal with an intracellular excess of ROS [29]. Three types of enzymes are key in this process: superoxide dismutases catalyze the dismutation of superoxide into O_2 and H_2O_2, and catalases and peroxiredoxins detoxify H_2O_2 by enzymatic degradation [14]. As a complementary strategy, cells express polyenes in their envelope to form a protective shield that quenches ROS, thereby preventing their entry into the cell [11, 26]. One of the most well-known groups of pigments with a polyene chromophore that display antioxidant activity are the carotenoids. While their functional analogy to APEs in bacterial protection from ROS has been recognized [1, 4], carotenoids are produced by a biosynthetically distinct process. These lipophilic isoprenoids are assembled from isopentenyl pyrophosphate and dimethylallyl pyrophosphate building blocks by the subsequent action of a prenyl transferase, phytoene synthase and phytoene desaturase [30]. Examples of bacterial carotenoids that protect their producers from external ROS are the 'golden' pigment staphyloxanthin, produced by *S. aureus* (Fig. 1) and the red pigment deinoxanthin from *Deinococcus radiodurans* [11, 26, 31]. Amide-containing polyenes are a different family of pigments that are present in Gram-positive cell envelopes. These compounds are produced by a fatty-acid-like type II polyketide pathway more closely related to APE biosynthesis. The red pigment granadaene is an ornithine rhamno-polyene produced by group B *Streptococcus* and it has been implicated in oxidative stress protection (Fig. 1, [10, 12]). A related compound was isolated from *Propionibacterium jensenii* [32] and a related BGC from commensal *Lactobacillus reuteri* was shown to produce a polyenic small molecule that stimulates the host aryl hydrocarbon receptor [33]. A potential role in bacterial protection from ROS remains to be investigated for the latter two examples. We challenged APE_{Ec} expressing bacteria with various concentrations of H_2O_2 and found that they significantly increased survival compared to the control strain (Fig. 4). Our results are corroborated by other studies showing that APEs protect from oxidative stress in a variety of different bacterial genera, including *Variovorax* [4], *Lysobacter* [6] and *Xanthomonas* [34-36]. Carotenoids and amide-containing polyenes present an interesting example of convergent evolution in Gram-positive bacteria and our results suggest an analogous function for APEs in Gram-negative bacteria.

Laboratory strains of *E. coli* K-12 are typically poor biofilm formers [37]. It was therefore surprising that heterologous expression of the APE_{Ec} BGC from the UPEC strain CFT073 in Top10 resulted in a robust increase in biofilm formation. There are various cell-envelope associated factors that contribute to *E. coli* adhesion to solid surfaces and biofilm formation, including type 1 and curli fimbriae, conjugative pili, autotransporters, cell surface polysaccharides, and capsules [37-39]. The mechanism by which APE_{Ec} expression contributes to the biofilm formation process remains to be determined. If APEs are part of a larger glycolipid molecule, it is possible that the cell surface localization of this molecular entity structurally supports the polysaccharide matrix. Alternatively, APE expression could cause a change of the outer membrane that results in increased exposure of previously characterized cell-surface adhesion factors.

Uropathogenic *E. coli*, such as the APE_{Ec} parent strain CFT073, display a biofilm-like phenotype during urinary tract infection (UTI) [40]. After colonization of the urethra, bacteria ascend to the bladder where they can invade epithelial cells. The intracellular bacteria then replicate rapidly and form biofilm-like intracellular bacterial communities that can remain stable for multiple weeks, even after a standard course of oral antibiotic treatment has been completed. These bacteria can flux out of the epithelial cells in large numbers and cause the infection to resurge, and potentially ascend to the kidneys, thereby causing a more severe disease state such as pyelonephritis. The partly intracellular lifestyle of UPEC makes treatment challenging, since antibiotics cannot penetrate into the epithelial cells and the treatment regimen might be shorter than the time the

bacteria persist intracellularly [41]. In addition, biofilm formation on indwelling devices, such as stents, implants, and catheters can form reservoirs of pathogenic bacteria thus leading to chronic infections. Catheter-associated urinary tract infections are the most common hospital acquired infections in the USA, and UPEC strains are the predominant cause [42]. Interestingly, overexpression of the transcriptional regulator TosR in *E. coli* CFT073 caused increased biofilm formation, as well as induced expression of the APE_{Ec} BGC [43], though no functional link between these two events has yet been established. Our future studies will focus on the antioxidant and biofilm-inducing roles of APEs in the context of *in vivo* bacterial pathogenesis.

Several examples exist within the Enterobacteriaceae, where APE BGCs are located on pathogenicity islands [1, 44, 45], suggesting they could be transmitted to other bacteria through horizontal gene transfer. This potential mobility is a major concern, especially given their roles in protection from oxidative stress and biofilm formation. It is therefore important to gain a fundamental understanding of APE biosynthesis and biology, in order to develop APE-targeting strategies for combating multidrug-resistant pathogens and preventing their biofilm formation.

Collectively, our data demonstrated the importance of studying the *in vivo* production of APEs, highlighting key differences not appreciable using elegant *in vitro* systems. Moreover, we have demonstrated a potential role for APEs in the pathogenic function of Gram-negative Enterobacteriaceae, mediating resistance to oxidative stress and facilitating robust biofilm formation. Our work provides essential molecular detail that could advance efforts to develop much-need therapeutic strategies to treat pathogenic *E. coli*.

METHODS

General methods, bacterial cultures and growth media

E. coli cultures were grown as liquid or solid agar media, using a Luria-Bertani or Mueller-Hinton base. Incubation was at 37°C, except for the strains that required 28°C incubation because they contain a plasmid with temperature sensitive ori. Antibiotic concentrations used for selection and maintenance were carbenicillin (100 µg/ml), kanamycin (50 µg/ml) and apramycin (50 µg/ml). Plasmid DNA isolation was performed with a standard kit according to the manufacturer's instructions (Qiagen). General microbiological manipulations, PCR amplification, cloning and transformation procedures were as described previously [46]. Enzymes were purchased from New England Biolabs, and chemicals from MilliporeSigma or Fisher Scientific, unless otherwise stated. Oligonucleotide primers were obtained from Integrated DNA Technologies.

In-frame scarred mutant construction

The bacterial strains, primers and plasmids used or generated in this study are listed in Tables S1-3. Individual genes in the APE_{Ec} BGC were replaced with an 81 bp in-frame scar sequence in a two-step PCR-generated recombineering process [25]. The procedure is illustrated schematically in Fig. S1 for *apeK*, other genes were replaced in an analogous manner. pJC121 is the parent plasmid that was used for generating all Δscar derivatives ([1], Table S3). Briefly, in the first step, a targeting cassette is generated by PCR amplification of the FRT sites that flank the apramycin resistance gene from pIJ773. The primers used for amplification contain large (on average 58 nt) 5' tales that are homologous to the up and downstream regions of the gene to be deleted (Table S2). The pIJ121 parent vector and targeting cassette are introduced into *E. coli* BW25113 with pIJ790 (a λRED recombination plasmid) and the genes of interest are replaced with the $apra^R$ marker via double homologous recombination, yielding the respective $\Delta apra^R$

constructs for each gene (even numbered plasmids pJC130-164 in Table S3). In the second step, the resistance markers are removed by introducing the Δapra^R plasmids into *E. coli* BT340. Expression of Flp recombinase by this strain causes recombination of the FRT sites that flank the apra^R marker, leaving an 81 bp scar sequence. The resulting in-frame scarred mutant plasmids can be identified based on their apramycin sensitivity (odd numbered plasmids PJC131-165 in Table S3).

H_2O_2 survival and MIC assays

For H_2O_2 survival assays, a starter culture was grown overnight in LB, cells were pelleted and resuspended in PBS at OD_{600} = 1. Equal volumes of H_2O_2 (in PBS) were added, final concentrations ranging from 0 to 7 mM. Reactions were incubated for 1 hour, quenched by addition of excess catalase and serially diluted prior to plating onto LB agar. Colony forming units were counted after overnight incubation at 37°C and percent survival was calculated relative to the PBS only control. To determine the MICs for H_2O_2 against APE$^+$ and APE$^-$ strains, a starter culture was grown overnight in LB. This was diluted to OD_{600} = 0.1 and used to inoculate the experimental cultures 1:10 into fresh LB medium containing serially diluted H_2O_2, final concentrations ranging from 0 to 100 µM. MICs were determined after 24 hours static incubation at 37°C.

E. coli biofilm assays

An overnight culture of APE$^+$ and APE$^-$ *E. coli* was adjusted to OD_{600} = 1, and 10 µl was used to inoculate a total of 1 ml fresh medium in flat-bottom, non-tissue culture treated plates. Biofilms were grown by static incubation at 37°C for 48 or 72 hours. All steps were performed with care to not disturb the biofilms. After removing the supernatant, cells were fixed for 30 minutes with 250 µl Bouin's solution (Sigma). The fixing solution was removed and cells were washed twice with 250 µl sterile H_2O prior to staining for quantification or confocal imaging. For quantitative staining, fixed samples were submerged in 250 µl of a 0.1% v/v crystal violet solution for 15 minutes. The staining solution was removed and samples were washed twice with 250 µl sterile H_2O. The remaining material was dissolved in 300 µl of 95% v/v ethanol, and quantified by measuring absorbance at 595 nm. Fixed biofilm samples that were processed for confocal imaging were stained with 250 µl of SYTO 9 green fluorescent dye. Confocal laser scanning microscopy image acquisition was performed using a Leica TCS SP5, using the 20× objective. Volocity (Quorum Technologies) was used to measure biofilm thickness and to produce three-dimensional rendered images by combining z-stacked images that were recorded at a z-step of 0.25 µm.

REFERENCES

1. Cimermancic, P., et al., *Insights into secondary metabolism from a global analysis of prokaryotic biosynthetic gene clusters.* Cell, 2014. **158**(2): p. 412-21.
2. Xu, H., et al., *Innate immune sensing of bacterial modifications of Rho GTPases by the Pyrin inflammasome.* Nature, 2014. **513**(7517): p. 237-41.
3. Drevinek, P. and E. Mahenthiralingam, *Burkholderia cenocepacia in cystic fibrosis: epidemiology and molecular mechanisms of virulence.* Clin Microbiol Infect, 2010. **16**(7): p. 821-30.

4. Schoner, T.A., et al., *Aryl Polyenes, a Highly Abundant Class of Bacterial Natural Products, Are Functionally Related to Antioxidative Carotenoids.* Chembiochem, 2016. **17**(3): p. 247-53.
5. Reichenbach, H., et al., *Flexirubin-type pigments in Flavobacterium.* Archives of Microbiology, 1980. **126**(3): p. 291-293.
6. Wang, Y., et al., *Biosynthetic mechanism for sunscreens of the biocontrol agent Lysobacter enzymogenes.* PLoS One, 2013. **8**(6): p. e66633.
7. Jenkins, C.L. and M.P. Starr, *The pigment ofXanthomonas populi is a nonbrominated aryl-heptaene belonging to xanthomonadin pigment group 11.* Current Microbiology, 1982. **7**(4): p. 195-198.
8. Grammbitter, G.L.C., et al., *An Uncommon Type II PKS Catalyzes Biosynthesis of Aryl Polyene Pigments.* J Am Chem Soc, 2019.
9. Pelz, A., et al., *Structure and biosynthesis of staphyloxanthin from Staphylococcus aureus.* J Biol Chem, 2005. **280**(37): p. 32493-8.
10. Rosa-Fraile, M., et al., *Granadaene: proposed structure of the group B Streptococcus polyenic pigment.* Appl Environ Microbiol, 2006. **72**(9): p. 6367-70.
11. Clauditz, A., et al., *Staphyloxanthin plays a role in the fitness of Staphylococcus aureus and its ability to cope with oxidative stress.* Infect Immun, 2006. **74**(8): p. 4950-3.
12. Liu, G.Y., et al., *Sword and shield: linked group B streptococcal beta-hemolysin/cytolysin and carotenoid pigment function to subvert host phagocyte defense.* Proc Natl Acad Sci U S A, 2004. **101**(40): p. 14491-6.
13. Forman, H.J. and M. Torres, *Reactive oxygen species and cell signaling: respiratory burst in macrophage signaling.* Am J Respir Crit Care Med, 2002. **166**(12 Pt 2): p. S4-8.
14. Fang, F.C., *Antimicrobial actions of reactive oxygen species.* mBio, 2011. **2**(5).
15. Fang, F.C., *Antimicrobial reactive oxygen and nitrogen species: concepts and controversies.* Nat Rev Microbiol, 2004. **2**(10): p. 820-32.
16. Liu, C.I., et al., *A cholesterol biosynthesis inhibitor blocks Staphylococcus aureus virulence.* Science, 2008. **319**(5868): p. 1391-4.
17. Flemming, H.C., et al., *Biofilms: an emergent form of bacterial life.* Nat Rev Microbiol, 2016. **14**(9): p. 563-75.
18. Costerton, J.W., P.S. Stewart, and E.P. Greenberg, *Bacterial biofilms: a common cause of persistent infections.* Science, 1999. **284**(5418): p. 1318-22.
19. Lewis, K., *Riddle of biofilm resistance.* Antimicrob Agents Chemother, 2001. **45**(4): p. 999-1007.
20. Nichols, B.P. and J.M. Green, *Cloning and sequencing of Escherichia coli ubiC and purification of chorismate lyase.* J Bacteriol, 1992. **174**(16): p. 5309-16.
21. De Lay, N.R. and J.E. Cronan, *A genome rearrangement has orphaned the Escherichia coli K-12 AcpT phosphopantetheinyl transferase from its cognate Escherichia coli O157:H7 substrates.* Mol Microbiol, 2006. **61**(1): p. 232-42.
22. Powers, M.J. and M.S. Trent, *Intermembrane transport: Glycerophospholipid homeostasis of the Gram-negative cell envelope.* Proc Natl Acad Sci U S A, 2019. **116**(35): p. 17147-17155.
23. Viljoen, A., et al., *The diverse family of MmpL transporters in mycobacteria: from regulation to antimicrobial developments.* Mol Microbiol, 2017. **104**(6): p. 889-904.
24. Konovalova, A. and T.J. Silhavy, *Outer membrane lipoprotein biogenesis: Lol is not the end.* Philos Trans R Soc Lond B Biol Sci, 2015. **370**(1679).
25. Gust, B., et al., *PCR-targeted Streptomyces gene replacement identifies a protein domain needed for biosynthesis of the sesquiterpene soil odor geosmin.* Proc Natl Acad Sci U S A, 2003. **100**(4): p. 1541-6.
26. Liu, G.Y., et al., *Staphylococcus aureus golden pigment impairs neutrophil killing and promotes virulence through its antioxidant activity.* J Exp Med, 2005. **202**(2): p. 209-15.

27. De Lay, N.R. and J.E. Cronan, *In vivo functional analyses of the type II acyl carrier proteins of fatty acid biosynthesis.* J Biol Chem, 2007. **282**(28): p. 20319-28.
28. Goel, A.K., et al., *Genetic locus encoding functions involved in biosynthesis and outer membrane localization of xanthomonadin in Xanthomonas oryzae pv. oryzae.* J Bacteriol, 2002. **184**(13): p. 3539-48.
29. Imlay, J.A., *Diagnosing oxidative stress in bacteria: not as easy as you might think.* Curr Opin Microbiol, 2015. **24**: p. 124-31.
30. Armstrong, G.A., *Genetics of eubacterial carotenoid biosynthesis: a colorful tale.* Annu Rev Microbiol, 1997. **51**: p. 629-59.
31. Tian, B., et al., *Evaluation of the antioxidant effects of carotenoids from Deinococcus radiodurans through targeted mutagenesis, chemiluminescence, and DNA damage analyses.* Biochim Biophys Acta, 2007. **1770**(6): p. 902-11.
32. Vanberg, C., et al., *Propionibacterium jensenii produces the polyene pigment granadaene and has hemolytic properties similar to those of Streptococcus agalactiae.* Appl Environ Microbiol, 2007. **73**(17): p. 5501-6.
33. Ozcam, M., et al., *Gut Symbionts Lactobacillus reuteri R2lc and 2010 Encode a Polyketide Synthase Cluster That Activates the Mammalian Aryl Hydrocarbon Receptor.* Appl Environ Microbiol, 2019. **85**(10).
34. He, Y.W., et al., *Xanthomonas campestris diffusible factor is 3-hydroxybenzoic acid and is associated with xanthomonadin biosynthesis, cell viability, antioxidant activity, and systemic invasion.* Mol Plant Microbe Interact, 2011. **24**(8): p. 948-57.
35. Poplawsky, A.R., S.C. Urban, and W. Chun, *Biological role of xanthomonadin pigments in Xanthomonas campestris pv. campestris.* Appl Environ Microbiol, 2000. **66**(12): p. 5123-7.
36. Rajagopal, L., et al., *The bacterial pigment xanthomonadin offers protection against photodamage.* FEBS Lett, 1997. **415**(2): p. 125-8.
37. Beloin, C., A. Roux, and J.M. Ghigo, *Escherichia coli biofilms.* Curr Top Microbiol Immunol, 2008. **322**: p. 249-89.
38. Niba, E.T., et al., *A genome-wide approach to identify the genes involved in biofilm formation in E. coli.* DNA Res, 2007. **14**(6): p. 237-46.
39. Pratt, L.A. and R. Kolter, *Genetic analysis of Escherichia coli biofilm formation: roles of flagella, motility, chemotaxis and type I pili.* Mol Microbiol, 1998. **30**(2): p. 285-93.
40. Flores-Mireles, A.L., et al., *Urinary tract infections: epidemiology, mechanisms of infection and treatment options.* Nat Rev Microbiol, 2015. **13**(5): p. 269-84.
41. Rosen, D.A., et al., *Detection of intracellular bacterial communities in human urinary tract infection.* PLoS Med, 2007. **4**(12): p. e329.
42. Ong, C.L., et al., *Identification of type 3 fimbriae in uropathogenic Escherichia coli reveals a role in biofilm formation.* J Bacteriol, 2008. **190**(3): p. 1054-63.
43. Luterbach, C.L., et al., *TosR-Mediated Regulation of Adhesins and Biofilm Formation in Uropathogenic Escherichia coli.* mSphere, 2018. **3**(3).
44. Lloyd, A.L., D.A. Rasko, and H.L. Mobley, *Defining genomic islands and uropathogen-specific genes in uropathogenic Escherichia coli.* J Bacteriol, 2007. **189**(9): p. 3532-46.
45. Lloyd, A.L., et al., *Genomic islands of uropathogenic Escherichia coli contribute to virulence.* J Bacteriol, 2009. **191**(11): p. 3469-81.
46. Sambrook, J., E.F. Fritsch, and T. Maniatis, *Molecular Cloning: a Laboratory Manual*. 1989, Cold Spring Harbor, N.Y: Cold Spring Harbor Laboratory Press.
47. Mobley, H.L., et al., *Pyelonephritogenic Escherichia coli and killing of cultured human renal proximal tubular epithelial cells: role of hemolysin in some strains.* Infect Immun, 1990. **58**(5): p. 1281-9.
48. Datsenko, K.A. and B.L. Wanner, *One-step inactivation of chromosomal genes in Escherichia coli K-12 using PCR products.* Proc Natl Acad Sci U S A, 2000. **97**(12): p. 6640-5.

49. Cherepanov, P.P. and W. Wackernagel, *Gene disruption in Escherichia coli: TcR and KmR cassettes with the option of Flp-catalyzed excision of the antibiotic-resistance determinant.* Gene, 1995. **158**(1): p. 9-14.

ACKNOWLEDGEMENTS

We thank Dr. John W Peterson and Dr. Judith A Drazba of the LRI imaging core for assistance with the biofilm imaging. **Funding:** JC is supported by seed funding from the Cleveland Clinic Foundation. This work was supported in part by National Institutes of Health grants R01 DK120679 (JMB), P50 AA024333 (JMB), and P01 HL147823 (JMB). **Author contributions:** Conceptualization and design: IJ, JC. Investigation: IJ, LJO, EAM, AK, KBS, JC. Figures: IJ, LJO, JC. Writing of the original draft: IJ, JC. Writing, review and interpretation: IJ, LJO, PPA, JMB, JC. **Competing interests:** none declared. **Materials and correspondence:** Please address all correspondence and material requests to JC at claesej@ccf.org

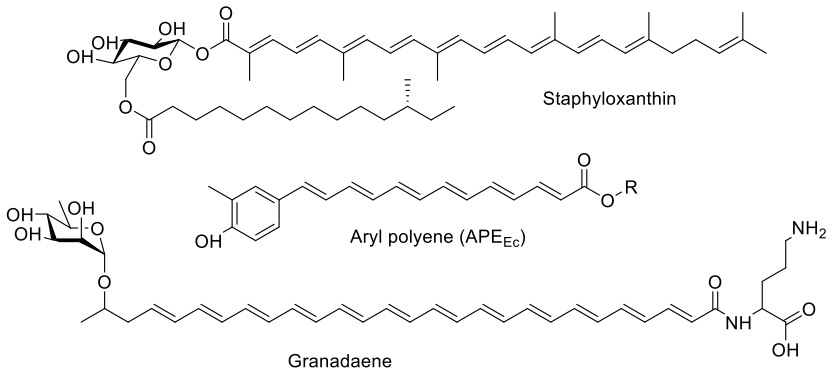

Figure 1. Chemical structures of pigmented fitness factors localized in the cell envelope of bacterial pathogens. Staphyloxanthin is the carotenoid produced by *S. aureus* responsible for the organism's characteristic golden color (top). Aryl polyenes are widespread yellow pigments among Gram-negative pathogens (middle), for example APE_{Ec} from uropathogenic *E. coli*. Granadaene is an ornithine rhamno-polyene that constitutes the red pigmentation in Group B *Streptococcus* (bottom) [1, 9, 10].

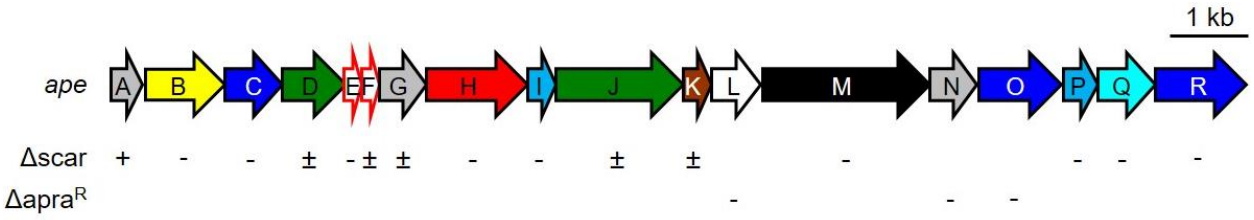

Figure 2. Pigmentation phenotype of individual deletion mutants in the APE_{Ec} BGC. Schematic arrow representation of the *E. coli* CFT073 APE_{Ec} BGC. The pigmentation phenotype of individual scarred deletion mutants (Δscar) is reported below the BGC as follows: + (wild-type level pigmentation), ± (reduced pigmentation), – (non-pigmented). We did not obtain scarred deletion mutants for *apaL*, *apeN* and *ape*O, and their respective $\Delta apra^R$ mutants are not pigmented, although this could be due to polar effects on downstream genes in the BGC.

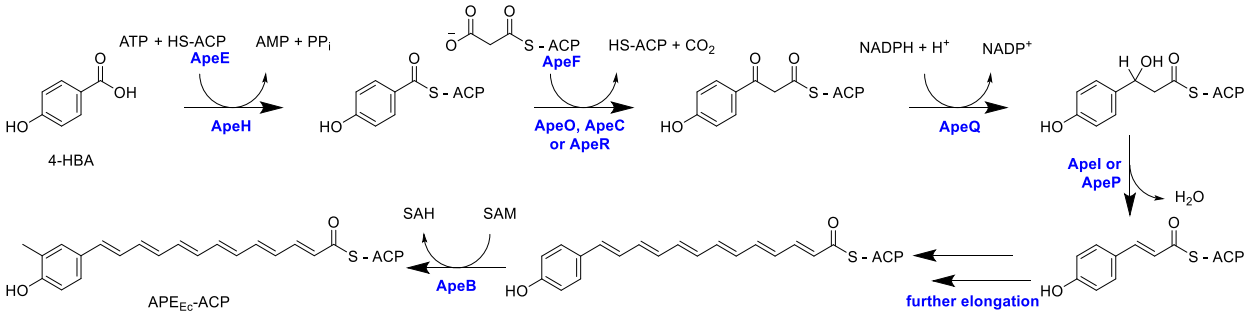

Figure 3. Proposed pathway for APE_{Ec} biosynthesis. APE_{Ec} biosynthesis is predicted to start with the ACP-activation of 4-hydroxybenzoic acid (4-HBA), an early intermediate in ubiquinone biosynthesis. The aromatic starter is further elongated with malonyl-ACP units by repetitive action of fatty-acid-like type II polyketide biosynthetic enzymes. The aromatic head group is methylated by ApeB and subsequently APE_{Ec} is predicted to be released from its ACP by a thioesterase, ApeK, and attached to a larger entity in the cell envelope by two acyltransferases, ApeD and ApeJ (not shown). Involvement of core enzymes in the pathway are indicated for *E. coli* CFT073 (in blue). SAM = *S*-adenosyl-L-methionine, SAH = *S*-adenosyl-L-homocysteine.

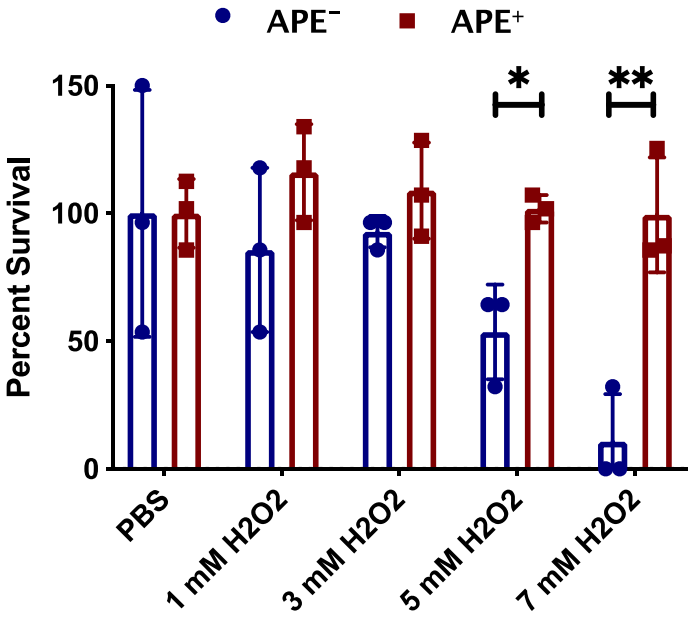

Figure 4. APE_{Ec} expression protects from oxidative challenge. Percent survival is calculated from colony forming units after a 60-minute H_2O_2 challenge for the APE_{Ec} expressing (APE^+) versus control strain (APE^-) relative to the PBS control. The reactions were stopped by adding an excess of catalase. PBS = phosphate buffered saline (n=3 repeats; error bars represent SD; *p<0.05 and **p<0.01 by unpaired, two-tailed t-test).

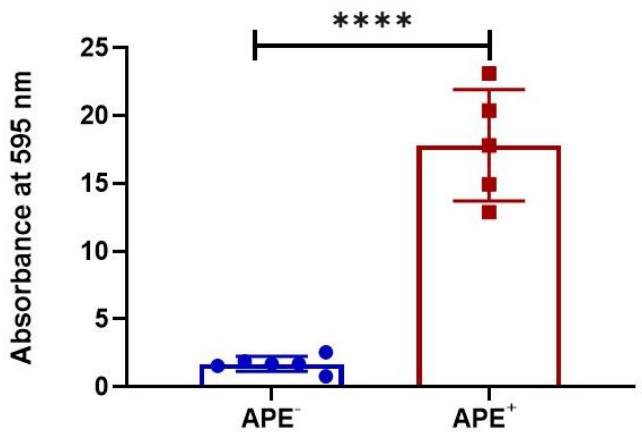

Figure 5. APE_{Ec} expression increases *E. coli* biofilm formation. Biofilms were grown in non-treated multi-well plates for 48 hours and subsequently stained with crystal violet. Absorbance at 595 nm was measured and normalized to APE^- values (n=6 repeats; error bars represent SD; ****p<0.0001 by unpaired, two-tailed t-test).

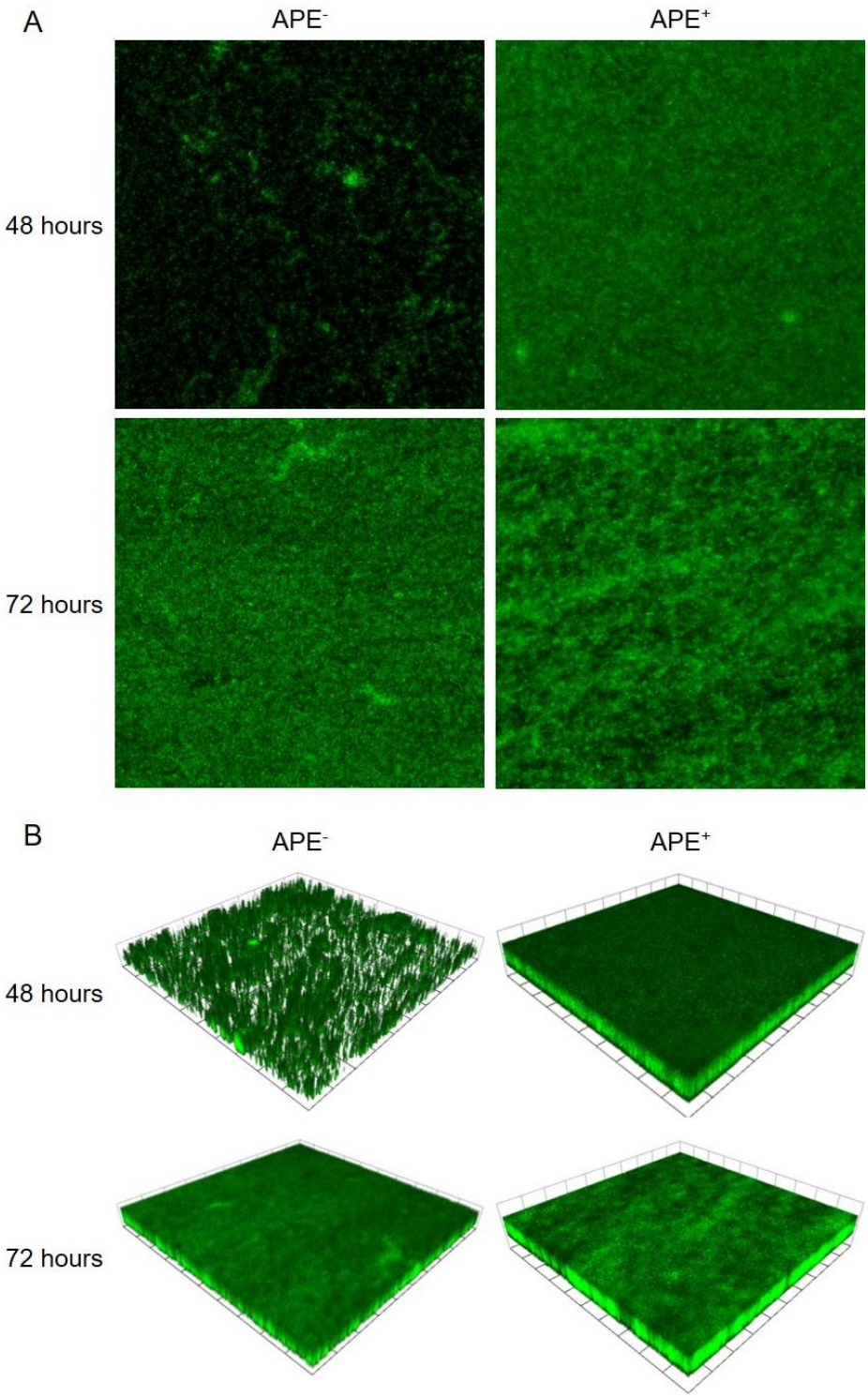

Figure 6. APE_{Ec} expressing *E. coli* more rapidly form thicker and denser biofilms. A) Confocal fluorescence microscopy images of APE^- and APE^+ *E. coli* biofilms that were grown in non-tissue culture treated multi-well plates for 48 hours and 72 hours. Samples were fixed, stained with SYTO 9, and imaged using the 63× objective. **B)** Three-dimensional rendering of the z-stacked images for the APE^- and APE^+ biofilms shows that APE_{Ec} expression results in formation of a thicker and denser biofilm. 1 scale unit = 57.97 µm.

Table 1. Predicted gene functions for the APE_{Ec} BGC.

ape	Locus tag	Predicted function
A	c1204	lipoprotein
B	c1203	SAM-dependent methyltransferase
C	c1202	3-ketoacyl-ACP synthase
D	c1201	(lyso)phospholipid acyltransferase
E	c1200	acyl carrier protein
F	c1199	acyl carrier protein
G	c1198	COG4648 - membrane protein
H	c1197	acyl-ACP synthetase
I	c1196	3-hydroxyacyl-ACP dehydratase
J	c1194	acyltransferase
K	c1193	thioesterase
L	c1192	outer membrane lipoprotein carrier
M	c1191	transporter
N	c1190	DUF3261 - membrane protein
O	c1189	3-ketoacyl-ACP synthase
P	c1188	3-hydroxyacyl-ACP dehydratase
Q	c1187	3-ketoacyl-ACP reductase
R	c1186	3-ketoacyl-ACP synthase